



Fabrication of Functional Materials for Dye-sensitized Solar Cells

Sarawut Tontapha^{1,2}, Pikaned Uppachai^{3,4*} and Vittaya Amornkitbamrung^{1,2,4*}

¹ Integrated Nanotechnology Research Center, Department of Physics, Faculty of Science, Khon Kaen University, Khon Kaen, Thailand, ² Institute of Nanomaterials Research and Innovation for Energy (IN-RIE), Khon Kaen University, Khon Kaen, Thailand, ³ Department of Applied Physics, Faculty of Engineering, Rajamangala University of Technology Isan, Khon Kaen, Thailand, ⁴ Center for Alternative Energy Research and Development, Faculty of Engineering, Khon Kaen University, Khon Kaen, Thailand

OPEN ACCESS

Edited by:

Su Pei Lim,
Xiamen University, Malaysia

Reviewed by:

Zhibin Yang,
Shanghai Jiao Tong University, China
Mingxing Wu,
Hebei Normal University, China

*Correspondence:

Pikaned Uppachai
pikaned.up@rmuti.ac.th
Vittaya Amornkitbamrung
vittaya@kku.ac.th

Specialty section:

This article was submitted to
Solar Energy,
a section of the journal
Frontiers in Energy Research

Received: 15 December 2020

Accepted: 31 March 2021

Published: 30 April 2021

Citation:

Tontapha S, Uppachai P and
Amornkitbamrung V (2021)
Fabrication of Functional Materials for
Dye-sensitized Solar Cells.
Front. Energy Res. 9:641983.
doi: 10.3389/fenrg.2021.641983

Dye-sensitized solar cells (DSSCs) have been developed as a promising photovoltaic cell type in recent decades because of their low cost, environmental friendliness, ease of fabrication, and suitability for a wide range of indoor and outdoor applications, especially under diverse shaded and low-light condition. They are typically composed of three main components: a transparent conducting oxide (TCO) substrate-based working electrode with wide-bandgap semiconductors and dye sensitizer molecules, an electrolytic mediator based on redox couple species, and a TCO-based counter electrode consisting of catalyst materials. The development of intrinsic and functional organic, inorganic, metal oxide, composite, and carbon-based materials has been intensively studied to enhance the efficiency of DSSCs. A simple and low-cost fabrication process that uses natural products is also considered essential for further large-scale production. In this article, we review the fabrication of various functional materials and their effects on DSSC performance.

Keywords: dye-sensitized solar cells, functional materials, carbon-based materials, composite materials, density functional theory

INTRODUCTION

Dye-sensitized solar cells (DSSCs) represent promising molecular architecture opportunities in the field of energy conversion. DSSCs consist of three crucial parts: a working electrode (WE) with a photosensitizer, an electrolytic mediator, and a counter electrode (CE).

The development of new photosensitizers for DSSCs is a challenge that is being pursued through investigations at the molecular level. Recently, dye molecules have been developed from natural and synthetic sources to allow practical implementation and have accordingly attracted the attention of numerous researchers seeking to develop materials with better photosensitizing properties. The sensitizer plays an essential role in light absorption and electron injection into the conduction band of a semiconductor.

In DSSCs, an electrolyte based on a tri-iodide/iodide (I_3^-/I^-) mediator provides the best electrochemical efficiency and is widely utilized with a metal catalyst. However, this electrolyte is extremely corrosive to the metal film catalyst of a CE (Olsen et al., 2000). Reducing the corrosive activity of iodide by using the highly stable catalyst materials is therefore a key to realizing the full potential of an I_3^-/I^- electrolyte. The use of an organic disulfide/thiolate (T_2/T^-) electrolyte has also been investigated because of its high transmittance and low corrosivity; it exhibits higher efficiency and stability than the conventional I_3^-/I^- electrolyte.

Since Pt-based CEs exhibit the best electrochemical efficiency, they are commonly used in high-performance DSSCs, but Pt is not the only catalyst that has been studied. Materials, such as conductive allotropes of carbon, graphite, graphene, and carbon nanotubes, as well as amorphous and diamond-like and graphite-like carbon composite films have also significantly advanced this field of research. Furthermore, high-performance catalysts using composite or functional materials have been developed to promote the greater surface area, low charge-transfer resistance, and cocatalytic activity.

To provide a clear picture of the progress of DSSC research, this review provides a summary of recent advances in the fabrication of DSSC components. Indeed, a great deal of research has been conducted to evaluate various WEs, photosensitizers, electrolytes, and CEs, as detailed in **Figure 1** and **Table 1**, and discussed in the following sections.

ADVANCED FUNCTIONAL MATERIALS FOR PHOTOELECTRODES

Metal Oxide and Nanocomposite Materials

Nanocrystalline TiO₂-based mesoporous electrodes are frequently used in DSSCs because TiO₂ exhibits the highest efficiency among the investigated materials, which also include ZnO, SnO₂, Nb₂O₅, SrTiO₃, Zn₂SnO₄, and ZnO-coated SnO₂ (Hagfeldt et al., 2010). In an efficient DSSC, the photoelectrode should have the following characteristics (Hasan et al., 2020):

- High surface area and porosity.
- A conduction band level should be sufficiently lower than the lowest unoccupied molecular orbital of the dye molecule.
- High electrical conductivity.
- Good chemical stability avoid photo- or chemical corrosion.
- The ability to absorb or scatter the solar radiation effectively.

The development of efficient WEs based on various types of materials is accordingly reviewed in this section. A modified photoelectrode was developed by adding nitrogen heterocycles as electron-donors, which produced a negative shift in the conduction band and reduced electron recombination (Lau and Soroush, 2019). Other additives in the semiconductor materials with a suitable cation/anion have also sufficient conduction band edge providing high electron injection rate (Hasan et al., 2020). A DSSC-based metal oxide semiconductor co-adsorbed with guanidinium [C(NH₂)₃⁺] cations achieved an efficiency of 11.04% (Grätzel, 2004). Furthermore, adding other cation dopants, such as Ni, W, Al, Nb, Sn, Li, Fe, Cu, Zn, Ce, La, and Eu, to semiconductor materials can change by the interfacial energy levels leading to faster electron hole separation from dye to mesoporous electrodes and also reduced the recombination of photoelectrons at the electrolyte–semiconductor interface (Watson and Meyer, 2004; Roose et al., 2015; Hasan et al., 2020). The anionic dopants, including N, B, C, S, P, F, I, and Br, have also been reported (Zhang et al., 2010; Cheng et al., 2015). In comparison to cationic dopants, anionic dopants have a greater electrical conductivity because of their superior thermal and photochemical stabilities (Hasan et al., 2020).

Besides cationic/anionic additives, Jarernboon et al. (2009a) studied the effects of multiwall carbon nanotubes (MWCNTs) on the reduction of the microcrack formation in metal oxide TiO₂ films. They successfully synthesized a nanocomposite TiO₂/MWCNT film using an electrophoretic deposition technique, finding that a minimal addition of MWCNTs to the TiO₂ solution significantly reduced the degree of TiO₂ cracking. It was suggested that MWCNTs minimize cracking by bonding to TiO₂ particles through the interaction of their hydroxyl and carboxylic groups. The spectrophotometric measurements revealed that the MWCNTs were well dispersed on the film, and the amount of MWCNTs incorporated on the film increased with increasing MWCNT concentration in the solution.

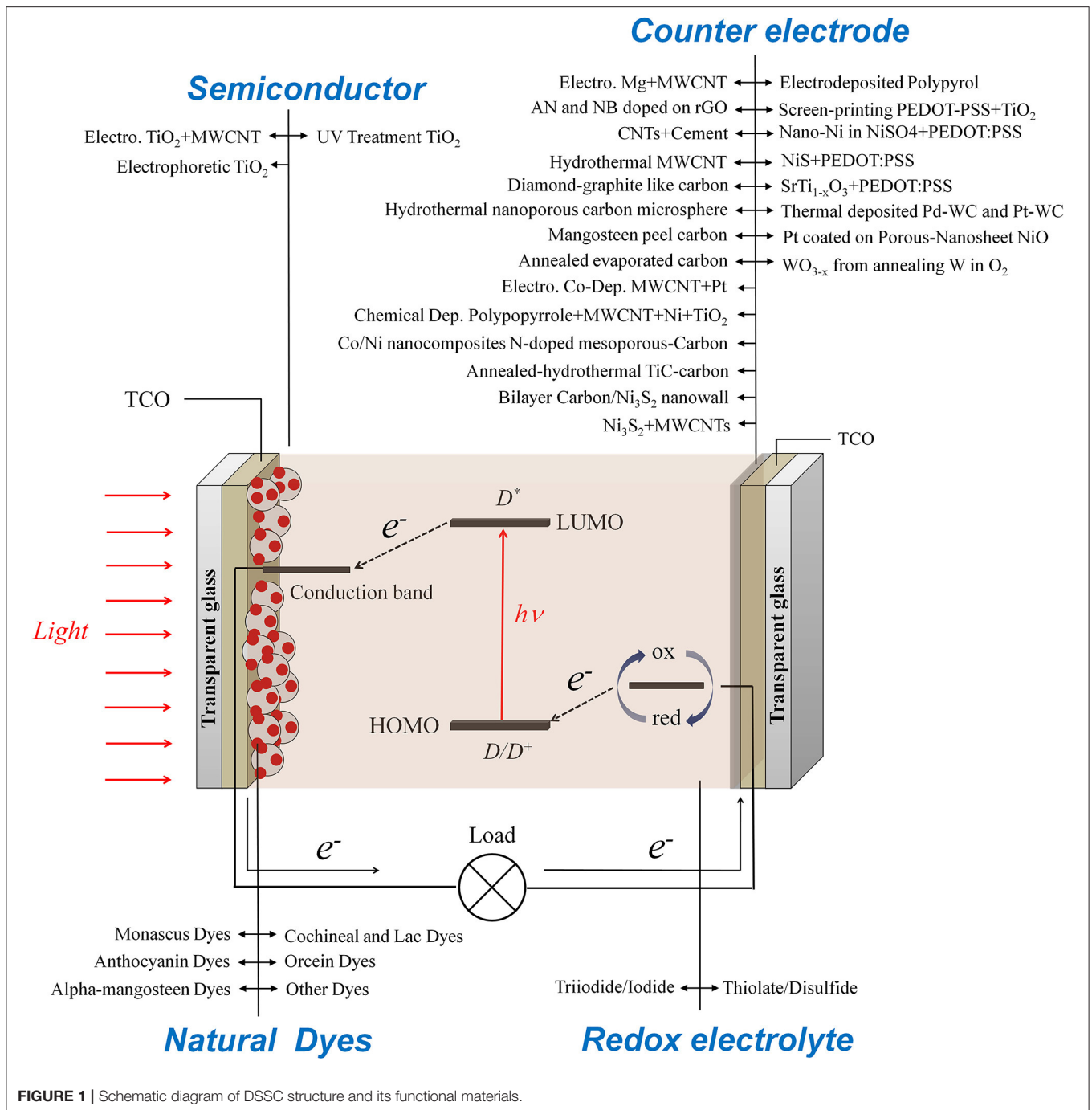
Jarernboon et al. (2009b) reported the optimization of TiO₂ films for DSSC applications prepared *via* electrophoretic deposition. It was found that the thickness of the TiO₂ films increased proportionally with the deposition time and voltage. However, as the deposition time or deposition voltage increased, the film surface became more discontinuous and microcracks became evident. The characteristics of these films as WEs were also analyzed. The energy conversion efficiency and photocurrent density were both dependent on TiO₂ thickness. The curve fitting of the relationship between energy conversion efficiency and TiO₂ thickness revealed an optimum solar cell efficiency of ~2.8% at a film thickness of ~14 μm.

Saekow et al. (2012) reported a huge increase in the photocurrent density and conversion efficiency of DSSCs manufactured using a high-intensity UV-O₃ treatment on TiO₂-layered WEs. This high-intensity UV-O₃ treatment reduces the charge-transfer resistance and increases the amount of dye adsorbed onto the TiO₂ surface. This appears to have the same effect as the sintering of electrical contacts through UV illumination during the manufacturing of the semiconductors.

Photosensitizer and Molecular Development

Photosensitizers are a critical component of DSSCs that play an essential role in light absorption and electron injection into the conduction band of a semiconductor. A dye sensitizer acts to absorb photons that contain energy equal to or higher than the energy gap of its molecules, improving the efficiency of DSSCs. Indeed, a sufficient driving force is required to convert light into electricity (Sang-aroon et al., 2019), providing an opportunity to design and develop molecular dyes for use as photosensitizers in DSSCs. Such dyes can either be derived from natural sources or be synthesized, and their molecular structures have been improved considerably by ongoing research. The molecular architecture of an effective photosensitizer has the following essential characteristics (Hagfeldt et al., 2010):

- The photosensitizer should have small molecules that are easily dispersed to cover the nanocluster surfaces of semiconductors and form many layers for adsorption.



- The absorption spectrum of the photosensitizer should cover the entire visible region and even part of the near-infrared (NIR) region.
- The photosensitizer should have many anchoring groups such as $-\text{OH}$, $-\text{COOH}$, $-\text{H}_2\text{PO}_3$, and $-\text{SO}_3\text{H}$, which can strongly bind to the semiconductor surface.
- The excited state of the photosensitizer should be higher in energy than the conduction band edge of the semiconductor, so that an efficient electron transfer process can occur between

- the excited dye and conduction band can occur. In contrast, the highest occupied molecular orbital of the photosensitizer should have a more positive potential than the valence band of the semiconductor.
- For dye regeneration, the oxidized state of the photosensitizer must be more positive than the redox potential of the electrolyte.
- Unfavorable dye aggregation on the semiconductor surface should be avoided by optimizing the molecular structure of the dye or by adding the co-adsorbents that prevent aggregation.

- *The photosensitizer should be photothermally and electrochemically stable.*

Many different sensitizing dyes, including synthetic dyes (i.e., metal complexes and metal-free organic dyes) and natural dye pigments, have been evaluated for the application as photosensitizers in DSSCs according to the requirements in the studies by Sang-aroon et al. (2012, 2013, 2014), Chaiamornnugool et al. (2017), Tontapha et al. (2017), and Phinjaturus et al. (2016). The theoretical calculations are an important tool that can be used to understand, express, predict, and optimize the properties of the photochemical mechanism of sensitizing dyes during the intramolecular transition. In particular, a fundamental understanding of density functional theory (DFT) is helpful for designing and developing molecular structures to achieve better photosensitizer efficiency. Therefore, the DFT and time-dependent DFT (TD-DFT) methods have been used to calculate and predict the geometric structures of different dyes and explain their interactions within DSSC cells at an electron scale (Sang-aroon et al., 2012, 2013, 2014; Chaiamornnugool et al., 2017; Tontapha et al., 2017).

Among the natural sensitizing dyes, monascus (Sang-aroon et al., 2012), cochineal and lac dyes (Sang-aroon et al., 2013), orcein dyes (Sang-aroon et al., 2014), anthocyanins (Maiaugree et al., 2015a; Phinjaturus et al., 2016; Chaiamornnugool et al., 2017; Tontapha et al., 2017), mangosteen dyes (Maiaugree et al., 2015a; Tontapha et al., 2017), and others (Sang-aroon et al., 2019) have shown good photosensitizing properties in both theoretical and experimental procedures. The main properties of DSSCs with various dye sensitizers are summarized in **Table 1**. However, the conversion efficiency of natural dyes when used as molecular sensitizers is still lower than that of synthetic dyes. Thus, it is necessary to search for new and highly effective synthetic dyes for the development of more effective photosensitive materials. Alternatively, the dye adsorption patterns can be designed with double- or triple-layered architectures to provide high-efficiency DSSCs. However, this is currently a challenge, as molecular engineering must be used to modify the electronic and molecular structures of the dyes to shift their absorption into the visible light region. Additionally, the adsorption kinetics of sensitizing dyes should be experimentally determined to develop an understanding of the adsorption rate of individual dyes.

ELECTROLYTES

Electrolytes are an important part of dye charge regeneration from its oxidized state to neutral state form by receiving electrons from redox mediators. The electrolyte-based redox couple system provides several benefits when applying an electrolyte to a device, such as (Krishna et al., 2019; Sang-aroon et al., 2019; Hasan et al., 2020):

- *Substantial ion mobility and low viscosity to support the fast transfer of electrons.*
- *A high diffusion coefficient.*
- *Long-term stability.*

- *Good interfacial contact with the nanocrystalline semiconductor and counter electrode.*
- *No tendency to induce dye desorption from the semiconductor surface or the dye degradation.*
- *Non-absorption in the visible light region.*

An I_3^-/I^- redox couple electrolyte is typically employed in DSSCs (Maiaugree et al., 2015a; Sang-aroon et al., 2019) as it provides the best electrochemical efficiency and is widely used with a metal film catalyst. However, an organic T_2/T^- electrolyte has also been used in a DSSC to take advantage of its high transmittance and low corrosivity (Towannang et al., 2012, 2015, 2018; Maiaugree et al., 2013, 2015a; Sang-aroon et al., 2019; Tangtrakarn et al., 2019; Tontapha et al., 2020). Indeed, an impressive efficiency of 2.63% for a DSSC-based T_2/T^- electrolyte was achieved with a natural dye sensitizer as studied by Maiaugree et al. (2015a).

Towannang et al. (2015) reported the performance of a DSSC employing a T_2/T^- electrolyte. In addition to theoretical calculations, our previous study showed that DFT can be used to investigate the electrocatalytic potentials as well as the energetic, electronic, and thermodynamic properties of CE-based monolayer graphene nanosheets (GNSs) reacted with the T_2/T^- electrolyte (Tontapha et al., 2020). It was found that GNSs can achieve high reactivity with electrolytes, making them an excellent candidate of electrocatalytic material for the design of high-performance DSSC CEs. However, other redox couples incorporated in the organic solutions, such as $SCN^-/(SCN)^{3-}$, S/S^{2-} , Ni^{3+}/Ni^{4+} , Cu^+/Cu^{2+} , and Co^{2+}/Co^{3+} , are also good electrolytes (Nusbaumer et al., 2001; Hattori et al., 2005; Nelson et al., 2008; Klahr and Hamann, 2009; Feldt et al., 2010; Li et al., 2010; Tsao et al., 2011; Kashif et al., 2012; Hasan et al., 2020). For example, the obtained efficiency of DSSC 13–14% was achieved by using cobalt-based electrolyte (Mathew et al., 2014; Kakiage et al., 2015).

ADVANCED FUNCTIONAL MATERIALS FOR COUNTER ELECTRODES

The development of catalyst materials with properties comparable with those of Pt is a crucial challenge in which the following characteristics must be attained:

- *Use of low-cost materials, such as carbon-based materials, metal oxides, metal carbides, metal sulfides, conductive polymers, and natural products.*
- *Use of low-cost, facile synthesis, and fabrication processes based on screen printing, doctor-blade application, hydrothermal deposition, and annealing processes.*
- *Use of cocatalyst materials as well as more active catalytic sites; that is, incorporating composites and dopants.*

Generally, carbon-based, metal-based, and composite-based CE materials have been investigated to achieve these characteristics.

Carbon and Carbon-based Materials

Allotropes of carbon have previously been reported as excellent catalysts because of their low cost, large surface area, high

TABLE 1 | Summary of the important results of DSSCs using functional natural sensitizer and carbon, carbon-based, metal-based, and composite-based CE materials.

Counter electrode	Dye-sensitizer	Electrolyte	J_{sc} (mA/cm ⁻²)	V_{oc} (V)	FF	PCE (%)	PCE/Pt (%)	References
Photosensitizer and molecular development								
Pt	Anthocyanins	I^-/I_3^-	2.91	0.46	0.53	n/a	0.71	Chaiamornnugool et al., 2017
Pt	α -mangostin	I^-/I_3^-	5.189	0.55	0.62	n/a	1.78	Tontapha et al., 2017
Pt	Anthocyanins	I^-/I_3^-	3.57	0.46	0.64	n/a	1.06	Phinjaturus et al., 2016
Carbon and carbon based materials								
Carbon black mixed graphite	N719	I^-/I_3^-	11.34	0.83	0.71	6.70	n/a	Kay and Grätzel, 1996
Carbon black	N719	I^-/I_3^-	16.80	0.79	0.69	9.10	n/a	Murakami et al., 2006
Electrospun carbon nanofibers	N719	I^-/I_3^-	12.60	0.76	0.57	5.50	6.97	Joshi et al., 2010
Sub-micrometer-sized graphite (CG-c)	N719	I^-/I_3^-	12.70	0.79	0.62	6.20	6.80	Veerappan et al., 2011
Graphene	N719	I^-/I_3^-	16.99	0.75	0.54	6.81	8.49	Zhang et al., 2011
SWCNT	N719	I^-/I_3^-	14.94	0.80	0.64	7.61	8.49	Zhang et al., 2011
DWCNT	N719	I^-/I_3^-	15.43	0.80	0.65	8.30	8.49	Zhang et al., 2011
MWCNT	N719	I^-/I_3^-	16.20	0.74	0.64	7.67	7.83	Lee et al., 2009
MWCNT	N719	I^-/I_3^-	15.25	0.80	0.56	7.06	8.49	Zhang et al., 2011
Mg incorporated MWCNT (W-Mg-0.04-g-CNT-1-min)	N719	I^-/I_3^-	3.71	0.67	0.43	1.08	n/a	Pimanpang et al., 2009
rGO	N719	I^-/I_3^-	12.58	0.70	0.58	5.11	7.89	Rakspun et al., 2020
AN-rGO (1:10)	N719	I^-/I_3^-	16.34	0.78	0.54	6.88	7.89	Rakspun et al., 2020
NB-rGO (1:10)	N719	I^-/I_3^-	15.92	0.72	0.62	7.11	7.89	Rakspun et al., 2020
rGO	N719	$[Co(bpy)_3]^{3+/2+}$	6.82	0.69	0.71	3.34	4.57	Rakspun et al., 2020
AN-rGO (1:10)	N719	$[Co(bpy)_3]^{3+/2+}$	10.20	0.67	0.65	4.44	4.57	Rakspun et al., 2020
NB-rGO (1:10)	N719	$[Co(bpy)_3]^{3+/2+}$	10.36	0.67	0.65	4.51	4.57	Rakspun et al., 2020
Cement:CNTs (29:71)	N719	I^-/I_3^-	18.66	0.80	0.64	9.60	11.22	Chindapasirt et al., 2019
Annealed-hydrothermal (AHT)-MWCNT	N719	I^-/I_3^-	14.27	0.78	0.68	7.66	8.01	Siroj et al., 2012
ITO/Pt/10 sccm N2 doped DLC	N719	I^-/I_3^-	2.33	0.58	0.34	1.85	3.20/3.53	Wang et al., 2011
600°C annealed DLC	N719	I^-/I_3^-	10.57	0.73	0.65	5.00	n/a	Park and Kim, 2011
500C-DLC	N719	I^-/I_3^-	15.70	0.74	0.66	7.61	7.74	Uppachai, 2015
Annealed-nanoporous carbon microspheres (A-CMS)	N719	I^-/I_3^-	16.82	0.80	0.57	7.71	8.05	Lowpa et al., 2015
Mangosteen peel carbon (MPC)	α -mangostin anthocyanins	T^-/T_2	8.70	0.60	0.50	2.63	1.47	Maiaugree et al., 2015a
Mangosteen peel carbon (MPC)	α -mangostin anthocyanins	I_2/NaI	5.58	0.70	0.51	1.99	1.75	Maiaugree et al., 2015b
Annealed-carbon	N719	I^-/I_3^-	18.56	0.74	0.64	8.74	8.80	Tangtrakarn et al., 2019
Annealed-carbon	N719	T^-/T_2	16.53	0.64	0.45	4.74	3.98	Tangtrakarn et al., 2019
PPy-MWCNTs	N719	I^-/I_3^-	14.99	0.71	0.62	6.56	7.20	Towannang et al., 2012
PPy-MWCNTs	N719	T^-/T_2	8.29	0.63	0.59	3.05	3.19	Towannang et al., 2012
MWCNTs/Pt	N719	I^-/I_3^-	16.10	0.77	0.71	8.90	8.13	Maiaugree et al., 2012a
Co-N-MC	N719	I^-/I_3^-	15.00	0.72	0.70	7.57	8.22	Hasin et al., 2017
Ni-N-MC	N719	I^-/I_3^-	16.60	0.73	0.70	8.42	8.22	Hasin et al., 2017
Co-N-MC	N719	T^-/T_2	16.00	0.70	0.60	6.80	5.25	Hasin et al., 2017
Ni-N-MC	N719	T^-/T_2	16.00	0.71	0.62	6.95	5.25	Hasin et al., 2017
Carbon/Ni ₃ S ₂	N719	I^-/I_3^-	20.75	0.75	0.62	9.64	8.38	Maiaugree et al., 2015b

(Continued)

TABLE 1 | Continued

Counter electrode	Dye-sensitizer	Electrolyte	J_{sc} (mA/cm ⁻²)	V_{oc} (V)	FF	PCE (%)	PCE/Pt (%)	References
AH-TiC-carbon	N719	T^-/T_2	10.12	0.65	0.55	3.59	3.84	Towannang et al., 2015
Ni ₃ S ₂ @MWCNTs	N719	I^-/I_3^-	17.25	0.75	0.56	7.48	7.24	Maiaugree et al., 2019
Metal-based and composite materials								
PVP-capped Pt	N719	I^-/I_3^-	10.50	0.65	0.41	2.84	2.79	Wei et al., 2006
PANI	N719	I^-/I_3^-	14.60	0.71	0.69	7.15	6.90	Li et al., 2008
PPy	N719	I^-/I_3^-	15.01	0.74	0.69	7.66	6.90	Wu et al., 2008
MWCNT/PEDOT:PSS	N719	I^-/I_3^-	15.5	0.66	0.63	6.50	8.50	Fan et al., 2008
AC-1R-PPy	N719	I^-/I_3^-	14.58	0.74	0.43	4.72	7.59	Keothongkham et al., 2012
PEDOT-PSS-30L (30% large TiO ₂ : 70% small TiO ₂)	N719	I^-/I_3^-	17.30	0.73	0.67	8.49	7.50	Maiaugree et al., 2012b
NiSO ₄ -PEDOT:PSS	N719	T^-/T_2	8.79	0.65	0.54	3.05	3.64	Maiaugree et al., 2013
0.3NiS(NPs)/PEDOT-PSS	N719	I^-/I_3^-	16.05	0.76	0.67	8.18	8.62	Maiaugree et al., 2017
STO_Co 0.075	N719	I^-/I_3^-	21.22	0.71	0.55	8.39	8.27	Maiaugree et al., 2018
Pt-WC	N719	T^-/T_2	11.93	0.60	0.59	4.29	3.80	Towannang et al., 2018
Pd-WC	N719	T^-/T_2	11.79	0.60	0.29	2.01	1.46 (Pd)	Towannang et al., 2018
FTO/PNO/Pt	N719	T^-/T_2	17.16	0.69	0.69	8.17	7.23	Maiaugree et al., 2014
WO _{2.6}	N719	I^-/I_3^-	13.44	0.76	0.51	5.25	6.96	Uppachai et al., 2014

corrosion resistance toward iodine, high reactivity for triiodide reduction, and suitable chemical compatibility with other elements (Grätzel, 2003). The use of magnesium nanoparticles and molecular dopants such as aniline (AN) and nitrobenzene (NB) on carbon nanostructures can provide high-performance catalysts for DSSCs based on iodide and cobalt-based electrolytes (Pimanpang et al., 2009; Rakspun et al., 2020). Furthermore, mixed powders containing MWCNTs and cement were coated onto a fluorine-doped tin oxide (FTO) substrate at a 29:71 ratio using a simple painting method without heating, resulting in a greater efficiency (9.60%) than that of a pure carbon DSSC (4.99%) (Chindapasirt et al., 2019).

An annealing treatment is commonly proposed to improve the electrical and electrocatalytic activities of DSSC materials. Siriraj et al. (2012) reported that hydrothermally depositing MWCNT onto a CE annealed at 180°C improved the efficiency of the DSSC from 2.37% (non-annealed) to 7.66%. Wang et al. (2011) reported that a DSSC using N-doped resistive diamond-like carbon (DLC) films as a catalyst exhibited an efficiency of only 1.57%; however, Park and Kim (2011) reported that the efficiency of a DSSC with a DLC film increased to 5% when using a 600°C annealing treatment on the DLC film. Similarly, the diamond-like and graphite-like composited films obtained by annealing a hydrogenated DLC film have been applied as efficient catalysts (Uppachai, 2015); annealing a DLC film at 500°C increased DSSC efficiency from 0.24 to 7.61%.

Nanoporous carbon microspheres (CMS) have been synthesized using a hydrothermal deposition method with carrot juice as the natural carbon source. An annealing process was then performed to increase the conductivity and surface area (149.10 m²/g) of the resulting microspheres. The efficiency of the

cell using this CMS CE was 0.17% before annealing and 7.71% after annealing (Lowpa et al., 2015). Maiaugree et al. (2015a) synthesized a mangosteen peel carbon (MPC) using a sintering process and applied it as a catalyst with a large surface area of 125 m²/g, in a DSSC comprising a T₂/T⁻ electrolyte. The efficiency of this DSSC reached 2.63%, which was higher than that of a DSSC with a Pt CE (1.47%).

The electrocatalytic activities of the T₂/T⁻ electrolyte and non-metal catalysts have also been investigated. Tangtrakarn et al. (2019) synthesized a post-annealed evaporated-carbon CE for a DSSC with a T₂/T⁻ electrolyte, achieving a solar efficiency of 8.04%. A short-term stability test was also performed over 50 days; the efficiency of the carbon DSSC was observed to remain constant, whereas that of the Pt DSSC decreased by 26%.

A cofunctioning catalyst was proposed to further enhance the electrocatalytic activity and surface area of the CE, resulting in improved solar cell performance. Enhanced DSSC performance was obtained by Towannang et al. (2012) and Maiaugree et al. (2012a) by using a polypyrrole (PPy) cocatalyst mixed with MWCNTs and MWCNTs/Pt, respectively. Similarly, the efficiency of a DSSC using an I₃⁻/I⁻ or T₂/T⁻ electrolyte was found to increase with the addition of the nanoparticle composites of cobalt or nickel to N-doped mesoporous carbon (Hasin et al., 2017). A pronounced 3.59% improvement in performance, close to that of a Pt DSSC (3.84%), was achieved by compositing TiC with carbon as the catalyst (Towannang et al., 2012). Furthermore, a combination of chemical bath deposition, an arc evaporation process, and annealing was used to synthesize a bilayered carbon-decorated Ni₃S₂ composite nanowall film as a cocatalyst (Maiaugree et al., 2015b). The large surface area of the nanostructure and its high electrocatalytic activity improved

the efficiency of a pure evaporated-carbon DSSC. The increased active surface area of nickel sulfide (Ni_3S_2) nanoparticles coated on MWCNTs prepared using a hydrothermal deposition process was also found to enhance DSSC performance (Maiaugree et al., 2019).

Metal-based and Composite Materials

An advantage of metal-based and composite CE cocatalyst materials is that they can be used in DSSCs instead of a pure PPy or PEDOT:PSS conductive polymer (Wu et al., 2008; Keothongkham et al., 2012). The composite catalyst materials, such as PEDOT:PSS+ TiO_2 (Maiaugree et al., 2012b), NiSO_4 +PEDOT:PSS (Maiaugree et al., 2013), NiS +PEDOT:PSS (Maiaugree et al., 2017), and $\text{SrTi}_{1-x}\text{O}_3$ +PEDOT:PSS (Maiaugree et al., 2018), have been prepared by using various methods employing doctor-blade applications, electrodeposition, or hydrothermal deposition processes. The efficiencies of DSSCs employing these composite materials were found to be significantly increased because multiple catalysts were excited. Towannang et al. (2018) used a hydrothermal process to fabricate a tungsten carbide (WC) CE catalyst with Pt or Pd particles for DSSCs with a T_2/T^- electrolyte, resulting in considerably improved cell efficiency. Maiaugree et al. (2014) synthesized the connected networks of sputtered Pt on porous nickel oxide (PNO) nanosheets for use as a catalyst. The solar conversion efficiency of the FTO/PNO/Pt DSSC was 8.17% compared to the 7.23% efficiency of the FTO/Pt DSSC, as the electrocatalytic activities were enhanced and the electroactive areas were increased. A tungsten oxide (WO_{3-x}) CE was easily prepared via thermal annealing of a tungsten sheet under a low-pressure O_2 atmosphere (Uppachai et al., 2014); the resulting presence of W^{6+} , W^{5+} , and W^{4+} valence states in the sub-stoichiometric WO_{3-x} produced excellent catalytic activity and electrical conductivity.

REFERENCES

- Amornkitbamrung, V., Pimanpang, S., Uppachai, P., and Faibut, N. (2015). *Catalytic Carbon Counter Electrode for Dye-Sensitized Solar Cells*. WIPO(PCT) No. WO2015116007A1. Bangkok: Axis Associates International Co., Ltd.
- Chaiamornnugool, P., Tontapha, S., Phatchana, R., Ratchapolthavisin, N., Kanokmedhakul, S., Sang-aroon, W., et al. (2017). Performance and stability of low-cost dye-sensitized solar cell based crude and pre-concentrated anthocyanins: combined experimental and DFT/TDDFT study. *J. Mol. Struct.* 1127, 145–155. doi: 10.1016/j.molstruc.2016.07.086
- Cheng, J., Chen, J., Lin, W., Liu, Y., and Kong, Y. (2015). Improved visible light photocatalytic activity of fluorine and nitrogen co-doped TiO_2 with tunable nanoparticle size. *Appl. Surf. Sci.* 332, 573–580. doi: 10.1016/j.apsusc.2015.01.218
- Chindapasirt, P., Jerernboon, W., Amornkitbamrung, V., and Ratchapolthavisin, N. (2019). *Carbon Nanotube-Cement Composite Composition for Catalysis on Counter Electrodes of Dye Sensitized Solar Cells*. JP Patent No. 6522152B2. Bangkok: Axis Associates International Co., Ltd.
- Fan, B., Mei, X., Sun, K., and Ouyang, J. (2008). Conducting polymer/carbon nanotube composite as counter electrode of dye-sensitized solar cells. *Appl. Phys. Lett.* 93:143103. doi: 10.1063/1.2996270
- Feldt, S. M., Gibson, E. A., Gabrielson, E., Sun, L., Boschloo, G., and Hagfeldt, A. (2010). Design of organic dyes and cobalt polypyridine redox mediators for high-efficiency dye sensitized solar cells. *J. Am. Chem. Soc.* 132, 16714–16724. doi: 10.1021/ja1088869
- Grätzel, M. (2003). Dye-sensitized solar cells. *J. Photochem. Photobiol. C* 4, 145–153. doi: 10.1016/S1389-5567(03)00026-1
- Grätzel, M. (2004). Conversion of sunlight to electric power by nanocrystalline dye sensitized solar cells. *J. Photochem. Photobiol. A* 164, 3–14. doi: 10.1016/j.jphotochem.2004.02.023
- Hagfeldt, A., Boschloo, G., Sun, L., Kloo, L., and Pettersson, H. (2010). Dye-sensitized solar cells. *Chem. Rev.* 110, 6595–6663. doi: 10.1021/cr900356p
- Hasan, M. M., Islam Md, D., and Rashid, T. U. (2020). Biopolymer-based electrolytes for dye-sensitized solar cells: a critical review. *Energy Fuels* 34, 15634–15671. doi: 10.1021/acs.energyfuels.0c03396
- Hasin, P., Amornkitbamrung, V., and Chanlek, N. (2017). Economical nanocomposites of cobalt or nickel species and polyaniline-derived N-doped mesoporous carbons for dye-sensitized solar cells as counter electrodes. *J. Catal.* 351, 19–32. doi: 10.1016/j.jcat.2017.03.021
- Hattori, S., Wada, Y., Yanagida, S., and Fukuzumi, S. (2005). Blue copper model complexes with distorted tetragonal geometry acting as effective electron-transfer mediators in dye-sensitized solar cells. *J. Am. Chem. Soc.* 127, 9648–9654. doi: 10.1021/ja0506814
- Jarernboon, W., Pimanpang, S., Maensiri, S., Swatsitang, E., and Amornkitbamrung, V. (2009a). Effects of multiwall carbon nanotubes in reducing microcrack formation on electrochemically deposited TiO_2 film. *J. Alloys Compd.* 476, 840–846. doi: 10.1016/j.jallcom.2008.09.157

CONCLUSIONS

Functional materials based on cost-effective and low-cost substrates, produced using practical and facile fabrication processes, can be transferred to large-scale DSSC production with optimized materials, components, and manufacturing processes (Amornkitbamrung et al., 2015; Chindapasirt et al., 2019). Co-catalysts and composite materials that provide low resistivity, high catalytic activity, and large surface area are particularly promising. The low-cost approaches using facile fabrication processes detailed in this review can reduce production time while remaining environmentally friendly.

AUTHOR CONTRIBUTIONS

VA: conceptualization and supervision. PU and ST: manuscript preparation and revision. All authors have read and agreed to the published version of the manuscript.

FUNDING

This work was supported by the Post-doctoral Training Program for Research Affairs and the Graduate School of Khon Kaen University (Grant no. 60166).

ACKNOWLEDGMENTS

The Institute of Nanomaterials Research and Innovation for Energy of the Department of Physics, Faculty of Science at Khon Kaen University, and the Center for Alternative Energy Research and Development at Khon Kaen University are gratefully acknowledged. The use of the research facilities at the Faculty of Engineering on the Khon Kaen campus of Rajamangala University of Technology Isan, is also acknowledged.

- Jarernboon, W., Pimanpang, S., Maensiri, S., Swatsitang, E., and Amornkitbamrung, V. (2009b). Optimization of titanium dioxide film prepared by electrophoretic deposition for dye-sensitized solar cell application. *Thin Solid Film* 517, 4663–4667. doi: 10.1016/j.tsf.2009.02.129
- Joshi, P., Zhang, L., Chen, Q., Galipeau, D., Fong, H., and Qiao, Q. (2010). Electrospun carbon nanofibers as low-cost counter electrode for dye-sensitized solar cells. *ACS Appl. Mater. Interfaces* 2, 3572–3577. doi: 10.1021/am100742s
- Kakiage, K., Aoyama, Y., Yano, T., Oya, K., Fujisawa, J. I., and Hanaya, M. (2015). Highly efficient dye-sensitized solar cells with collaborative sensitization by silyl-anchor and carboxy-anchor dyes. *Chem. Commun.* 51, 15894–15897. doi: 10.1039/C5CC06759F
- Kashif, M. K., Axelson, J. C., Duffy, N. W., Forsyth, C. M., Chang, C. J., Long, J. R., et al. (2012). A new direction in dye-sensitized solar cells redox mediator development: in situ fine-tuning of the cobalt(II)/(III) redox potential through Lewis base interactions. *J. Am. Chem. Soc.* 134, 16646–16653. doi: 10.1021/ja305897k
- Kay, A., and Grätzel, M. (1996). Low cost photovoltaic modules based on dye sensitized nanocrystalline titanium dioxide and carbon powder. *Sol. Energy Mater. Sol.* 44, 99–117. doi: 10.1016/0927-0248(96)00063-3
- Keothongkham, K., Pimanpang, S., Maiaugree, W., Saekow, S., Jarernboon, W., and Amornkitbamrung, V. (2012). Electrochemically deposited polypyrrole for dye-sensitized solar cell counter electrodes. *Int. J. Photoenergy* 2012:671326. doi: 10.1155/2012/671326
- Klahr, B. M., and Hamann, T. W. (2009). Performance enhancement and limitations of cobalt bipyridyl redox shuttles in dye-sensitized solar cells. *J. Phys. Chem. C* 113, 14040–14045. doi: 10.1021/jp903431s
- Krishna, J. V. S., Mrinalini, M., Prasanthkumar, S., and Giribabu, L. (2019). “Recent advances on porphyrin dyes for dye-sensitized solar cells,” in *Dye-Sensitized Solar Cells: Mathematical Modelling, and Materials Design and Optimization*, eds M. Soroush, and K. K. S. Lau (London: Academic Press), 231–284. doi: 10.1016/B978-0-12-814541-8.00007-0
- Lau, K. K. S., and Soroush, M. (2019). “Overview of dye-sensitized solar cells,” in *Dye-Sensitized Solar Cells Mathematical Modeling, and Materials Design and Optimization*, eds M. Soroush, and K. K. S. Lau (London: Academic Press), 1–49. doi: 10.1016/B978-0-12-814541-8.00001-X
- Lee, W. J., Ramasamy, E., Lee, D. Y., and Song, J. S. (2009). Efficient dye-sensitized solar cells with catalytic multiwall carbon nanotube counter electrodes. *ACS Appl. Mater. Interfaces* 1, 1145–1149. doi: 10.1021/am800249k
- Li, Q., Wu, J., Tang, Q., Lan, Z., Li, P., Lin, J., et al. (2008). Application of microporous polyaniline counter electrode for dye-sensitized solar cells. *Electrochem. Commun.* 10, 1299–1302. doi: 10.1016/j.elecom.2008.06.029
- Li, T. C., Spokoiny, A. M., She, C., Farha, O. K., Mirkin, C. A., Marks, T. J., et al. (2010). Ni(III)/(IV) bis(dicarbollide) as a fast, noncorrosive redox shuttle for dye-sensitized solar cells. *J. Am. Chem. Soc.* 132, 4580–4582. doi: 10.1021/ja100396n
- Lowpa, S., Pimanpang, S., Maiaugree, W., Saekow, S., Uppachai, P., Mitravong, S., et al. (2015). Nanoporous carbon microspheres from carrot juice used as a counter electrode for a dye-sensitized solar cell. *Matter. Lett.* 158, 115–118. doi: 10.1016/j.matlet.2015.05.039
- Maiaugree, W., Karaphun, A., Pimsawad, A., Amornkitbamrung, V., and Swatsitang, E. (2018). Influence of SrTi_{1-x}Co_xO₃ NPs on electrocatalytic activity of SrTi_{1-x}Co_xO₃ NPs/PEDOT-PSS counter electrodes for high efficiency dye sensitized solar cells. *Energy* 154, 182–189. doi: 10.1016/j.energy.2018.04.122
- Maiaugree, W., Kongprakaiwoot, N., Tangtrakarn, A., Saekow, S., Pimanpang, S., and Amornkitbamrung, V. (2014). Efficiency enhancement for dye-sensitized solar cells with a porous NiO/Pt counter electrode. *Appl. Surf. Sci.* 289, 72–76. doi: 10.1016/j.apsusc.2013.10.100
- Maiaugree, W., Lowpa, S., Towannang, M., Rutphonsan, P., Tangtrakarn, A., Pimanpang, S., et al. (2015a). A dye sensitized solar cell using natural counter electrode and natural dye derived from mangosteen peel waste. *Sci. Rep.* 5, 1–12. doi: 10.1038/srep15230
- Maiaugree, W., Pimanpang, S., Towannang, M., Rutphonsan, P., Laupa, S., Jarernboon, W., et al. (2012a). Co-electrophoretic deposition multiwall carbon nanotubes/Pt counter electrodes for dye-sensitized solar cell. *Jpn. J. Appl. Phys.* 51:10NE20. doi: 10.1143/JJAP.51.10NE20
- Maiaugree, W., Pimanpang, S., Towannang, M., Saekow, S., Jarernboon, W., and Amornkitbamrung, V. (2012b). Optimization of TiO₂ nanoparticle mixed PEDOT-PSS counter electrodes for high efficiency dye sensitized solar cell. *J. Non Cryst. Solids* 358, 2489–2495. doi: 10.1016/j.jnoncrysol.2011.12.104
- Maiaugree, W., Pimparue, P., Jarernboon, W., Pimanpang, S., Amornkitbamrung, V., and Swatsitang, E. (2017). NiS(NPs)-PEDOT-PSS composite counter electrode for a high efficiency dye sensitized solar cell. *Mat. Sci. Eng. B* 2017, 66–72. doi: 10.1016/j.mseb.2017.03.006
- Maiaugree, W., Tangtrakarn, A., Lowpa, S., Ratchapothavisin, N., and Amornkitbamrung, V. (2015b). Facile synthesis of bilayer carbon/Ni₃S₂ nanowalls for a counter electrode of dye-sensitized solar cell. *Electrochim. Acta* 174, 955–962. doi: 10.1016/j.electacta.2015.06.051
- Maiaugree, W., Tansoontona, T., Amornkitbamrun, V., and Swatsitanga, E. (2019). Ni₃S₂@MWCNTs films for effective counter electrodes of dye-sensitized solar cells. *Curr. Appl. Phys.* 19, 1355–1361. doi: 10.1016/j.cap.2019.08.020
- Maiaugree, W., Towannang, M., Thiangkaew, A., Harnchana, V., Jarernboon, W., Pimanpang, S., et al. (2013). Compositing NiSO₄ and PEDOT:PSS counter electrode for efficient dye-sensitized solar cell based on organic T₂/T⁻ electrolyte. *Matter. Lett.* 111, 197–200. doi: 10.1016/j.matlet.2013.08.084
- Mathew, S., Yella, A., Gao, P., Humphry-Baker, R., Curchod, B. F. E., Ashari-Astani, N., et al. (2014). Dye-sensitized solar cells with 13% efficiency achieved through the molecular engineering of porphyrin sensitizers. *Nat. Chem.* 6, 242–247. doi: 10.1038/nchem.1861
- Murakami, T. N., Ito, S., Wang, Q., Nazeeruddin Md, K., Bessho, T., Cesar, I., et al. (2006). Highly efficient dye-sensitized solar cells based on carbon black counter electrodes. *J. Electrochem. Soc.* 153, A2255–A2261. doi: 10.1149/1.2358087
- Nelson, J. J., Amick, T. J., and Elliott, C. M. (2008). Mass transport of polypyridyl cobalt complexes in dye-sensitized solar cells with mesoporous TiO₂ photoanodes. *J. Phys. Chem. C* 112, 18255–18263. doi: 10.1021/jp806479k
- Nusbaumer, H., Moser, J.-E., Zakeeruddin, S. M., Nazeeruddin, M. K., and Grätzel, M. (2001). Co^{II}(dcbp)₂²⁺ complex rivals tri-iodide/iodide redox mediator in dye-sensitized photovoltaic cells. *J. Phys. Chem. B* 105, 10461–10464. doi: 10.1021/jp012075a
- Olsen, E., Hagen, G., and Eric Lindquist, S. (2000). Dissolution of platinum in methoxy propionitrile containing LiI/I₂. *Sol. Energy Mater. Sol.* 63, 267–273. doi: 10.1016/S0927-0248(00)00033-7
- Park, Y. S., and Kim, H. K. (2011). The effects of annealing temperature on the characteristics of carbon counter electrodes for dye-sensitized solar cells. *Curr. Appl. Phys.* 11, 989–994. doi: 10.1016/j.cap.2011.01.004
- Phinjaturos, K., Maiaugree, W., Suriharn, B., Pimanpaeng, S., Amornkitbamrung, V., and Swatsitang, E. (2016). Dye-sensitized solar cells based on purple corn sensitizers. *Appl. Surf. Sci.* 380, 101–107. doi: 10.1016/j.apsusc.2016.02.050
- Pimanpang, S., Maiaugree, W., Jarernboon, W., Maensiri, S., and Amornkitbamrung, V. (2009). Influences of magnesium particles incorporated on electrophoretically multiwall carbon nanotube film on dye-sensitized solar cell performance. *Synth. Met.* 159, 1996–2000. doi: 10.1016/j.synthmet.2009.07.008
- Rakspun, J., Chiang, Y. J., Chen, J. Y., Yeh, C. Y., Amornkitbamrung, V., and Chanleke, N. (2020). Modification of reduced graphene oxide layers by electron-withdrawing/donating units on molecular dopants: facile metal-free counter electrode electrocatalysts for dye-sensitized solar cells. *Sol. Energy* 203, 175–186. doi: 10.1016/j.solener.2020.04.037
- Roose, B., Pathak, S., and Steiner, U. (2015). Doping of TiO₂ for sensitized solar cells. *Chem. Soc. Rev.* 44, 8326–8349. doi: 10.1039/C5CS00352K
- Saekow, S., Maiaugree, W., Jarernboon, W., Pimanpang, S., and Amornkitbamrung, V. (2012). High intensity UV radiation ozone treatment of nanocrystalline TiO₂ layers for high efficiency of dye-sensitized solar cells. *J. Non Cryst. Solids* 358, 2496–2500. doi: 10.1016/j.jnoncrysol.2012.01.050
- Sang-aroon, W., Kunmuak, K., Tontapha, S., Chaiamornnugool, P., Saekow, S., and Amornkitbamrung, V. (2014). Theoretical insight into electronic and photoelectrochemical properties of orcein dyes relevant to dye-sensitized solar cells. *Monatsh. Chem.* 145 1529–1537. doi: 10.1007/s00706-014-1237-2
- Sang-aroon, W., Laopha, S., Chaiamornnugool, P., Tontapha, S., Saekow, S., and Amornkitbamrung, V. (2013). DFT and TDDFT study on the electronic structure and photoelectrochemical properties of dyes derived from cochineal and lac insects as photosensitizer for dye-sensitized solar cells. *J. Mol. Model.* 19, 1407–1415. doi: 10.1007/s00894-012-1692-9
- Sang-aroon, W., Saekow, S., and Amornkitbamrung, V. (2012). Density functional theory study on the electronic structure of Monascus dyes as photosensitizer

- for dye-sensitized solar cells. *J. Photochem. Photobiol. A* 236, 35–40. doi: 10.1016/j.jphotochem.2012.03.014
- Sang-aroon, W., Tontapha, S., and Amornkitbamrung, V. (2019). "Photovoltaic performance of natural dyes for dye-sensitized solar cells: a combined experimental and theoretical study," in *Dye-Sensitized Solar Cells: Mathematical Modelling, and Materials Design and Optimization*, eds M. Soroush, and K. K. S. Lau (London: Academic Press), 203–229. doi: 10.1016/B978-0-12-814541-8.00006-9
- Siroj, S., Pimanpang, S., Towannang, M., Maiaugree, W., Phumying, S., Jarernboon, W., et al. (2012). High performance dye-sensitized solar cell based on hydrothermally deposited multiwall carbon nanotube counter electrode. *Appl. Phys. Lett.* 100:243303. doi: 10.1063/1.4726177
- Tangtrakarn, A., Maiaugree, W., Uppachai, P., Ratchapolthavisin, N., Moolsarn, K., Swatsitang, E., et al. (2019). High stability arc-evaporated carbon counter electrodes in a dye sensitized solar cell based on inorganic and organic redox mediators. *Diam. Relat. Mater.* 97:107451. doi: 10.1016/j.diamond.2019.107451
- Tontapha, S., Sang-aroon, W., Kanokmedhakul, S., Promgool, T., and Amornkitbamrung, V. (2017). Effects of dye-adsorption solvents, acidification and dye combination on efficiency of DSSCs sensitized by α -mangostin and anthocyanin from mangosteen pericarp. *J. Mater. Sci. Mater. Electron.* 28, 7454–7467. doi: 10.1007/s10854-017-6435-3
- Tontapha, S., Sang-aroon, W., Promgool, T., Kanokmedhakul, S., Maiaugree, W., Swatsitang, E., et al. (2020). Electrocatalytic activity of disulfide/thiolate with graphene nanosheets as an efficient counter electrode for DSSCs: a DFT study. *Mater. Today Commun.* 22:100742. doi: 10.1016/j.mtcomm.2019.100742
- Towannang, M., Kumlangwan, P., Maiaugree, W., Ratchaphonsaenwong, K., Harnchana, V., Jarernboon, W., et al. (2015). High efficiency organic-electrolyte DSSC based on hydrothermally deposited titanium carbide-carbon counter electrodes. *Electron. Mater. Lett.* 11, 643–649. doi: 10.1007/s13391-015-4411-8
- Towannang, M., Pimanpang, S., Thiangkaew, A., Rutphonsan, P., Maiaugree, W., Harnchana, V., et al. (2012). Chemically deposited polypyrrole-nanoparticle counter electrode for inorganic I^-/I_3^- organic T^-/T_2 dye-sensitized solar cells. *Synth. Met.* 162, 1954–1960. doi: 10.1016/j.synthmet.2012.08.017
- Towannang, M., Thiangkaew, A., Maiaugree, W., Ratchaphonsaenwong, K., Jarernboon, W., Pimanpang, S., et al. (2018). Thermally deposited palladium-tungsten carbide and platinum-tungsten carbide counter electrodes for a high performance dye-sensitized solar cell based on organic T^-/T_2 electrolyte. *J. Nanosci Nanotechnol.* 18, 1207–1214. doi: 10.1166/jnn.2018.13979
- Tsao, H. N., Yi, C., Moehl, T., Yum, J. H., Zakeeruddin, S. M., Nazeeruddin, M. K., et al. (2011). Cyclopenta dithiophene bridged donor-acceptor dyes achieve high power conversion efficiencies in dye-sensitized solar cells based on the tris-cobalt bipyridine redox couple. *Chem. Sus. Chem.* 4, 591–594. doi: 10.1002/cssc.201100120
- Uppachai, P. (2015). *High performance counter electrodes for dye-sensitized solar cells* (dissertation's thesis). Khon Kaen University, Khon Kaen, Thailand.
- Uppachai, P., Harnchana, V., Pimanpang, S., Amornkitbamrung, V., Brown, P. A., and Brydson, R. M. D. (2014). Substoichiometric tungsten oxide catalyst provides a sustainable and efficient counter electrode for dye-sensitized solar cells. *Electrochim. Acta* 145, 27–33. doi: 10.1016/j.electacta.2014.08.096
- Veerappan, G., Bojan, K., and Rhee, S. W. (2011). Sub-micrometer-sized graphite as a conducting and catalytic counter electrode for dye-sensitized solar cells. *ACS Appl. Mater. Interfaces* 3, 857–862. doi: 10.1021/am101204f
- Wang, S. F., Rao, K. K., Yang, T., and Wang, H. P. (2011). Investigation of nitrogen doped diamond like carbon films as counter electrodes in dye sensitized solar cells. *J. Alloys. Compd.* 509, 1969–1974. doi: 10.1016/j.jallcom.2010.10.103
- Watson, D. F., and Meyer, G. J. (2004). Cation effects in nanocrystalline solar cells. *Coord. Chem. Rev.* 248, 1391–1406. doi: 10.1016/j.ccr.2004.02.015
- Wei, T. C., Wan, C. C., and Wang, Y. Y. (2006). Poly(N-vinyl-2-pyrrolidone)-capped platinum nanoclusters on indium-tin oxide glass as counter electrode for dye-sensitized solar cells. *Appl. Phys. Lett.* 88:103122. doi: 10.1063/1.2186069
- Wu, J., Li, Q., Fan, L., Lan, Z., Li, P., Lin, J., et al. (2008). High-performance polypyrrole nanoparticles counter electrode for dye-sensitized solar cells. *J. Power Sources* 15, 172–176. doi: 10.1016/j.jpowsour.2008.03.029
- Zhang, D. W., Li, X. D., Li, H. B., Chen, S., Sun, Z., Yin, X. J., et al. (2011). Graphene-based counter electrode for dye-sensitized solar cells. *Carbon* 49, 5382–5388. doi: 10.1016/j.carbon.2011.08.005
- Zhang, J., Wu, Y., Xing, M., Leghari, S. A. K., and Sajjad, S. (2010). Development of modified N doped TiO_2 photocatalyst with metals, nonmetals and metal oxides. *Energy Environ. Sci.* 3, 715–726. doi: 10.1039/b927575d

Conflict of Interest: The authors declare that the research was conducted in the absence of any commercial or financial relationships that could be construed as a potential conflict of interest.

Copyright © 2021 Tontapha, Uppachai and Amornkitbamrung. This is an open-access article distributed under the terms of the Creative Commons Attribution License (CC BY). The use, distribution or reproduction in other forums is permitted, provided the original author(s) and the copyright owner(s) are credited and that the original publication in this journal is cited, in accordance with accepted academic practice. No use, distribution or reproduction is permitted which does not comply with these terms.